Electron spin resonance investigation of impurity and intrinsic defects in Nb-doped $BaTiO_3$ single crystal and ceramics

V. V. Laguta, A. M. Slipenyuk, I. P. Bykov, and M. D. Glinchuk
Institute for Problems of Material Science, NASc of Ukraine, 3 Krjijanovskogo Str, 03680 Kiev, Ukraine

M. Maglione
Institute of Condensed Matter Chemistry of Bordeaux - UPR 9048 CNRS 87, Av.Dr.Schweitzer F - 33608 PESSAC Cedex, France

A. G. Bilous and O. I. V'yunov
V.I.Vernadskii Institute of General and Inorganic Chemistry, NASc of Ukraine, 32/34 Palladina Ave, 03680, Kiev, Ukraine.

J. Rosa[a] and L. Jastrabik
Institute of Physics, Academy of Sciences of the Czech Republic, Na Slovance 2, 182 21 Prague 8, Czech Republic

(Received 30 June 2004; accepted 12 January 2005; published online 22 March 2005)

Electron spin resonance (ESR) spectra of impurity and intrinsic defects have been measured at 4.2–295 K in Nb-doped $BaTiO_3$ single crystals and ceramics to clarify their role in the conductivity and positive temperature coefficient of resistivity (PTCR effect). The measurements revealed a small amount of Fe^{3+}, Cr^{3+}, and Mn^{2+} impurities, which change their valence state (for example, $Cr^{5+} \rightarrow Cr^{3+}$, $Mn^{4+} \rightarrow Mn^{2+}$) with increased Nb concentration due to the compensation of the excess charge of Nb^{5+} ions. Besides the 3*d*-metal impurities, several types of Ti^{3+} polaronic and possible fluctuon states, where electrons can be localized near ferroelectric domain boundaries, have been revealed as well. All of them are associated with Ti^{3+} lattice ions and not with $Nb^{5+/4+}$ impurity, which apparently represents rather a very shallow donor level. The data obtained strongly support the polaronic origin of Nb-doped $BaTiO_3$ conductivity at $T<300$ K. Comparative investigations of ESR spectra in single crystals and ceramics of the same kind of $BaTiO_3$ together with computer simulation allowed us unambiguously to ascribe complex ESR signals observed in ceramic samples to Cr^{3+}, Mn^{2+}, and Fe^{3+} ions and Ti^{3+} polarons and/or fluctuons. The role of manganese ions at grain boundaries in the PTCR effect is discussed as well. © *2005 American Institute of Physics*. [DOI: 10.1063/1.1868856]

I. INTRODUCTION

In the past decade $BaTiO_3$ ceramics doped with Nb or rare-earth elements, which cause *n*-type conduction of this composition, became a subject of intense studies in order to explain the nature of the positive temperature coefficient of resistivity (PTCR effect) at temperatures close to the tetragonal-cubic phase transition T_c. This effect is useful for numerous technical applications, such as PTCR thermistors and heaters. The phenomenological understanding of the PTCR effect has been well defined on the basis of Heywang model[1] and later modifications of this concept.[2–5] However, the microscopical mechanism underlying the PTCR phenomenon is still poorly understood. In this respect, many reports were devoted to the role of various impurities and intrinsic defects in the transport properties of PTCR ceramics. In particular, it was found that the PTCR effect could be enhanced by the addition of small amounts of transition-metal elements such as Cu or Mn.[6,7] The 3*d*-metal ions substituted for Ti^{4+} are usually acceptors and, hence, act as traps for carriers. Doping with Nb leads to *n*-type conductivity of $BaTiO_3$. Thus, the Nb impurity acts as the source of conduction electrons. It is clear that the number of the conduction electrons depends not only on the concentration of Nb ions but also on the presence of unavoidable impurities in the lattice. These residual defects can compensate the excess charge of Nb^{5+} and, thus, decrease the number of free electrons in the conduction band. There is also an important question related to the role of unavoidable impurities and/or special dopants on the properties of grain boundaries, which must be nonconductive in the PTCR region. Therefore the study of the impurity subsystem together with intrinsic lattice defects, in which both can strongly influence the properties of the material, has been the key point in the physics of the semiconductive $BaTiO_3$, in particular on its conductivity and PTCR effect.

At low temperatures, the conductivity mechanism is essentially different from that in the vicinity of the PTCR temperature range. For $T<300$ K, the electrons are trapped on 3*d* metals deep levels which changes the type of conductivity. At rather low temperatures, the temperature dependence of the conductivity can be controlled by polaronic mechanism as has been claimed by several authors.[5,8] The microscopic mechanism of the electron polaron formation in $BaTiO_3$ lattice was recently established from electron spin

[a]Author to whom correspondence should be addressed; electronic mail: rosa@fzu.cz

TABLE I. Impurity content in pure and Cr-doped $BaTiO_3$ ceramics (mol %).

Element	$BaTiO_3$	$Ba(Ti_{0.999\,93}Cr_{0.000\,07})O_3$	$Ba(Ti_{0.999\,86}Cr_{0.000\,14})O_3$
Cr	0.0012(1)	0.007 5(8)	0.014(1)
Fe	0.018(2)	0.019(2)	0.011(1)
Mn	0.000 84(8)	0.000 49(5)	0.000 23(2)

resonance (ESR) studies, see Refs. 9 and 10. In particular, it was shown that a conduction electron has a strong tendency to be localized at Ti^{4+} lattice ions, creating Ti^{3+} small polarons. However, these studies were performed on undoped $BaTiO_3$ single crystals with a small concentration of Nb ($\sim$40–100 ppm), which was a background impurity.

In the present study, we are interested in the ESR investigation of both single crystals and ceramics of $BaTiO_3$ rather heavily doped with Nb (1000–4000 ppm or 0.1%–0.4% niobium in titanium site). These compounds are used in industrial applications and, thus, knowledge about impurities and lattice defects is particularly important. First, we present experimental results of the investigation of a single crystal sample. Then the spectral data obtained are used to analyze the ESR spectra in $BaTiO_3$ ceramic samples. A special attention was paid to Ti^{3+} related centers, whose ESR spectra were measured in both single crystals and ceramic samples of $BaTiO_3$.

II. EXPERIMENTAL DETAILS

A single crystal, with a nominal Nb concentration of 0.2%, has been grown by the top seeded solution method (for details see Ref. 11). In order to obtain Nb-doped crystals, Nb_2O_5 oxide has been introduced into the melt. The sample, of a characteristic transparent blue color, was not in a single domain state, because poling in a dc field was not possible owing to its relative high conductivity.

$BaTiO_3$ ceramic samples both pure and doped with Nb were fabricated by a conventional solid-phase reaction technique.[12] Extra-pure $BaCO_3$, TiO_2, SiO_2, Nb_2O_5 and water solution of ammonia were used as starting reagents. Powders were ball milled in agate mortar. Samples were calcinated at 1100–1200 °C. The chromium dopant in $BaTiO_3$ ceramic samples was precipitated from $CrCl_3$ solutions. Atomic emission spectroscopy analysis of undoped and Cr-doped $BaTiO_3$ samples showed the impurities listed in Table I. The densities of ceramic samples sintered at 1340–1360 °C in air were calculated by the Archimedes method and were found to be 92%–94% of the theoretical value. Electrophysical properties of samples have been investigated earlier and presented in Ref. 13.

Electron spin resonance (ESR) spectra were recorded in the temperature region 4.2–295 K using a spectrometer operating at microwave frequency 9.2–9.4 GHz.

III. EXPERIMENTAL RESULTS AND THEIR INTERPRETATION

A. ESR spectra in Nb-doped $BaTiO_3$ single crystal

Because of the high conductivity of Nb-doped $BaTiO_3$ crystals, ESR spectra were recorded below 100 K where the conductivity becomes low. As an example, in Fig. 1 we present such spectra taken at several temperatures. As can be seen from the figure, a spectrum of Cr^{3+} impurity is dominant at $T \approx 75$ K. ESR spectrum of the Cr^{3+} ions was identified by observation of the ^{53}Cr isotope hyperfine lines (see small intensity quartet in Fig. 1) and angular dependencies of the fine-transition resonance fields, which were described using well-known spectral parameters (see, for instance, Ref. 14). In Fig.1, one can see also three low-intensity lines out of the six lines, which belong to Mn^{2+} ions. Under temperature lowering, both the Cr^{3+} and Mn^{2+} spectra decrease in intensity and their line shape become asymmetric because the spin-lattice relaxation time increases and saturation effects begin to influence the line shape.

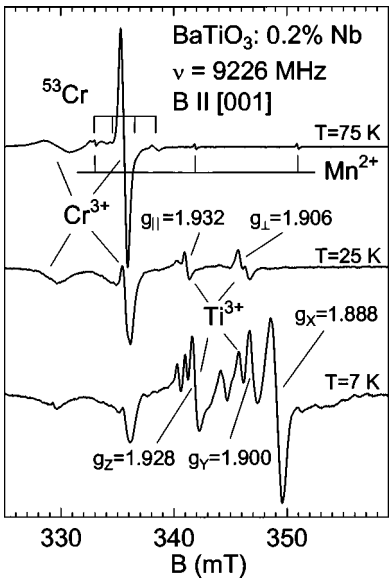

FIG. 1. ESR spectra in Nb-doped $BaTiO_3$ single crystal at several temperatures.

At $T < 30$ K, new ESR spectra appear in the g-factor region of 1.94–1.88. The feature of these resonances is very close to Ti^{3+} small polarons in undoped $BaTiO_3$ described earlier by Scharfschwerdt *et al.*[9] and Lenjer, Schirmer, and Hesse.[10] However, there are small differences in the Ti^{3+} g factors measured by us and those published in Refs. 9 and 10 (see Table II). In our opinion, these differences in the g-factor values may be due to the influence of internal stress induced by Nb impurity. As was shown in Ref. 10, Ti^{3+} small polaron spectra are very sensitive to the presence of external stress, which not only redistributes the population of localized electrons along the stress axis but also sizably shifts the g-factor values and changes the symmetry of the ground state.

Besides this spectrum a new type of ESR spectra arise at $T < 10$ K. Their intensity drastically rises with temperature lowering down to 3–4 K. Angular dependence of the resonance fields shows the presence of six equivalent centers of rhombic symmetry with principal axes along $\langle 100 \rangle$ cubic axes (Fig. 2). The angular dependencies, as in the case of Ti^{3+} small polarons, were described by a spin Hamiltonian for particles with a spin $S=1/2$ and following g factors: $g_x = 1.888$, $g_y = 1.900$, $g_z = 1.928$. These g factors are typical for

TABLE II. Principal g-factor values of the various Ti^{3+} related centers.

	g[100]	g[010]	g[001]	Remarks
Ti^{3+} (small polaron)	1.906(1)	1.906(1)	1.932(1)	Visible at $T \leqslant 35$ K
	1.907	1.907	1.936	$P=0$[a]
	1.898	1.898	Aligned	$P=0.24$ GPa[a]
Ti^{3+} ("intermediate" polaron or fluctuon)	1.888(1)	1.900(1)	1.928(1)	Visible at $T \leqslant 15$ K
	1.890	1.890	1.928	$P=0$[a]
	1.897	1.935	Aligned	$P=0.24$ GPa[a]
$Ti^{3+}-Nb^{5+}$	1.892	1.892	1.932	[a]

[a]Data from Ref. 10.

Ti^{3+} in a crystal field of distorted oxygen octahedron and, again, they are close to values previously ascribed in Ref. 10 to Ti^{3+} "intermediate" polarons, i.e., polarons with intermediate radius. It should be emphasized that the resonance lines measured by us are narrow; at $\mathbf{B}\|[001]$ the peak-to-peak linewidth is only about 0.8 mT, while the linewidth of Ti^{3+} intermediate polaron presented in Ref. 10 is almost ten times larger. Note also that both mentioned spectra differ by symmetry: the Ti^{3+} intermediate polaron spectrum has a tetragonal symmetry in contrast to the rhombic one measured by us. On the other hand, for such a broad line ($\sim$7 mT) of Ti^{3+} intermediate polaron it seems impossible to separate rather small splitting of ESR lines ($\sim$2 mT) corresponding to the g_x and g_y values. Another interesting fact is that the g_x and g_y values measured in our study are approximately equal to $g_\perp$ for Ti^{3+} intermediate polarons measured in Ref. 10 at pressure $P=0$ and 0.26 GPa, respectively (see Table I). Therefore, we cannot exclude that the spectrum revealed by us belongs to Ti^{3+} intermediate polaron as well. However, in our case, the Ti^{3+} polaron may be slightly perturbed by the presence of Nb^{5+} or other defect at a distance of 1–2 lattice constants, so that it will produce a rhombic distortion of the crystal field. This is in principle supported by the fact that the Nb impurities can influence only the g_x and g_y values because the g_z component changes only due to the perturbation of the upper E_g-symmetry $3d$ orbital states separated from the ground T_{2g} triplet by a large distance 25 000–30 000 cm^{-1}.[9]

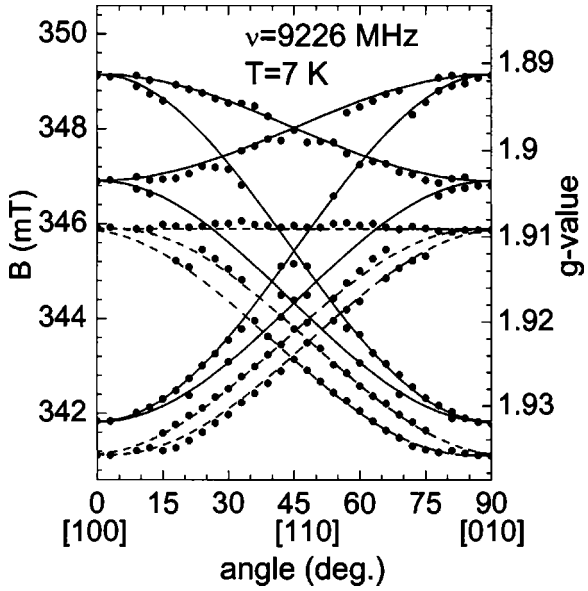

FIG. 2. Angular dependences of resonance magnetic fields of Ti^{3+} centers in Nb-doped $BaTiO_3$ single crystal measured at 7 K.

We now focus on the lack of hyperfine splitting of the ^{93}Nb ($I=9/2$) ESR lines. The reason could be the $|xy>$ symmetry of $3d^1$ orbital state (in this case an electronic density along $\langle 100 \rangle$ cubic axes is zero) as well as the rather large distance to next Ti positions (0.4 nm or more). On the other hand, we notice that the $Ti^{3+}-Nb^{5+}$ complex in $BaTiO_3$ had already been described (see Table II and Ref. 10). It differs slightly from our center by g factors and shows ^{93}Nb hyperfine structure. Therefore, at present the origin of our observed Ti^{3+} center is not completely clear.

It should be emphasized that in ferroelectrics there is also another possibility for conduction electrons to be localized, namely fluctuon-type localization, first introduced by Krivoglaz (see Ref. 15 and references therein). In particular, it was shown that the fluctuon type of carriers localization in ferroelectrics takes place near the domain boundaries, where fluctuation of polarization is large. It can happen in ferroelectrics at low temperatures, where the dielectric permittivity is small and anisotropic.[15] All these conditions are fulfilled in $BaTiO_3$ at least at $T \leqslant 100$ K. Moreover, impurities also promote the creation of fluctuons whose symmetry has to be lower than that of polaron. Therefore, keeping in mind the splitting of the ESR lines and the related three components of the g tensor, fluctuon-type of electron localization, rather than polaron one, can be supposed as well. The coexistence of tetragonal and rhombic symmetry spectra at $T=7$ K can result from the simultaneous polaron and fluctuon-type of electron localization. It should be mentioned that strong electron-phonon interaction involving critical point lattice polarization fluctuations associated with the soft TO mode was evidenced also from the electron mobility measurements in many perovskite oxides (e.g., $KTaO_3$, $SrTiO_3$, $BaTiO_3$).[16]

Let us also note that we did not observe, at least down to 3 K, "pure" Nb^{4+} centers in spite of rather high Nb doping. This means that the main part of the conduction electrons at low temperatures is localized at Ti sites as small and/or intermediate polarons or as fluctuons, in agreement with previous studies.[10,16]

B. ESR spectra in Nb-doped $BaTiO_3$ ceramics

ESR measurements at room temperature (RT) had shown the presence of several paramagnetic impurities in Nb-doped $BaTiO_3$ ceramics (Fig. 3). The intense spectra belong to Cr^{3+}

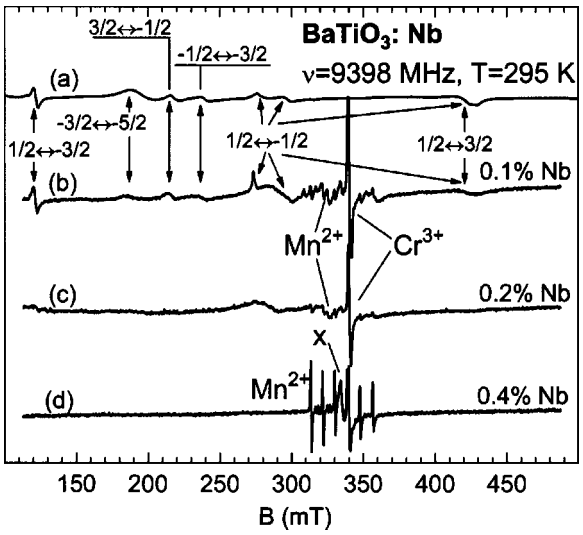

FIG. 3. ESR spectra in Nb-doped $BaTiO_3$ ceramics at several concentrations of niobium. Spectrum (a) is computer simulation of Fe^{3+} powder spectrum in the tetragonal phase.

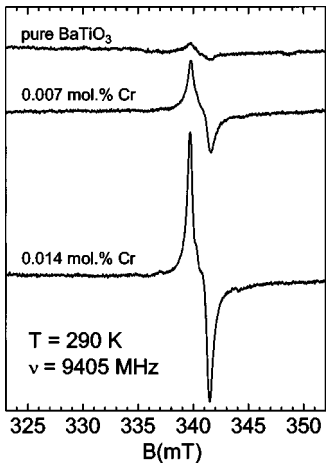

FIG. 5. Cr^{3+} ESR spectra in undoped and Cr-doped $BaTiO_3$ ceramics.

and Fe^{3+} ions. The assignment of the measured resonances to Fe^{3+} and Cr^{3+} impurities was made on the basis of the simulation of powder spectrum using spin Hamiltonian parameters found from single crystal measurements and reported, for instance, in Refs. 14, 17, and 18. The simulated and measured spectrum of Cr^{3+} in the field region of the $1/2 \leftrightarrow -1/2$ transition is presented in Fig. 4. In the simulation procedure we used numerical diagonalization of the spin Hamiltonians that allowed us to determine besides the resonance magnetic fields of all transitions (including forbidden ones), also their probabilities. However, for simplification of the computation, the same linewidth was taken for each of the fine transitions. Therefore, the relative intensities of different parts of the calculated powder spectrum do not exactly coincide with the measured ones. As an example, the simulated spectrum of Fe^{3+} is shown in Fig. 3(a). It is important to note that the intense line at $B \approx 120$ mT ($g \approx 5.8$) belongs to the $1/2 \leftrightarrow -3/2$ ($M=2$) Fe^{3+} forbidden transition and not to Fe^{3+}- oxygen vacancy (V_0) pair center as was assumed in Ref. 19 even if its g- factor is really close to that found for Fe^{3+}-V_0 centers in different ABO_3 lattices.[20] The relative intensity of the $1/2 \leftrightarrow -3/2$ transition line is large because its resonance field only slightly depends on crystallite orientation.

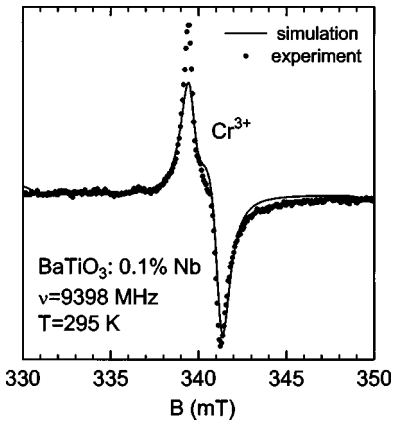

FIG. 4. Measured and simulated powder spectra of Cr^{3+} in the tetragonal phase.

We should note that several models and corresponding defect configurations were already proposed for the interpretation of the ESR signal at $g=1.971-1.974$ in $BaTiO_3$ ceramics. Among them we can mention the following: (i) intrinsic Ti^{3+}-related defects (Kutty, Murugaraj and Gajbhiye[21] and Er Ishida, and Takenchi[22]); (ii) barium vacancy (V_{Ba}) defect[23]); (iii) Cr^{3+} impurities.[24] To further prove our assignment of the ESR signal at $g=1.971-1.974$ to Cr^{3+} ions we performed measurements of $BaTiO_3$ ceramics specially sintered with different content of Cr impurity (20–80 at. ppm). The ESR spectrum observed at $g=1.971-1.974$ was completely identical to that of Nb-doped $BaTiO_3$ and the intensity of the signal increased proportionally to the chromium content rise (Fig. 5), which unambiguously proves our interpretation. Moreover, this spectrum was observed without any intensity decrease from 100 up to 400 K. In addition to Fe^{3+} and Cr^{3+} impurity ions, $BaTiO_3$:Nb ceramics also contained a small amount of Mn^{2+} impurity. Part of the Mn^{2+} resonance lines are visible in the vicinity of $g \approx 2$ (Fig. 3).

With increasing Nb concentration all spectra (Fe^{3+}, Cr^{3+}, and Mn^{2+}) change their intensities that reflect ionic valency change as the same raw materials of $BaCO_3$, TiO_2, and Nb_2O_5 were used for the ceramic samples preparation. Note that in undoped ceramics practically only the spectrum of Fe^{3+} is visible. This suggests that in undoped $BaTiO_3$ ceramics, manganese and chromium exist in the form of Mn^{3+} and Cr^{4+} or Mn^{4+} and Cr^{5+}, respectively. Thus, they are either ESR "silent" or not visible, at least at room temperatures, due to too short spin-lattice relaxation time. Low concentration Nb doping (<0.2 at. %) results in chromium and manganese valency change to the paramagnetic Cr^{3+} and Mn^{2+} states [Figs. 3(b) and 3(c)]. Such decrease of impurity charge-state is expected because Nb^{5+} substituting for Ti^{4+} brings a positive charge to the lattice. This tendency is also supported by the disappearance of the Fe^{3+} spectrum (due to a process $Fe^{3+}+e \rightarrow Fe^{2+}$) with Nb content increase. Heavily (more than 0.4 at. %) Nb-doped $BaTiO_3$ ceramics show only spectra of Cr^{3+} and Mn^{2+} ions and a signal X [Fig. 3(d)] that is often associated with singly ionized barium vacancy

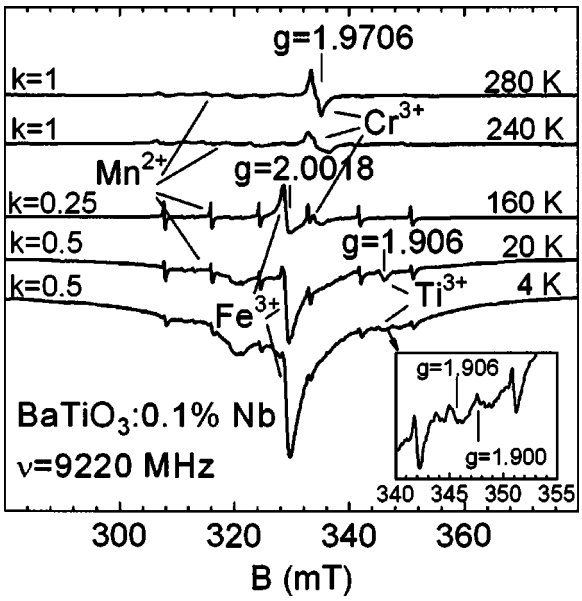

FIG. 6. Temperature dependence of ESR spectra in Nb-doped $BaTiO_3$ ceramics.

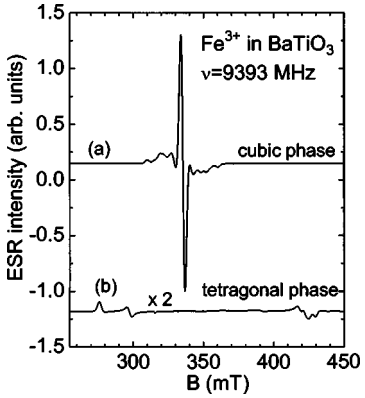

FIG. 7. Simulated powder spectra of Fe^{3+} in the magnetic field region of the $\pm 1/2$ central transition in (a) the cubic and (b) tetragonal phases, respectively. The spectrum (b) is magnified by a factor of 2 to be visible. The same linewidth was taken for both spectra.

$(V_{Ba}^{\bullet})$[21] or can be rather due to the presence of partly charged titanium vacancy (V_{Ti}^{III} defects).[25] However, here the Mn^{2+} spectrum completely changed. Instead of a tetragonal-symmetry spectrum [Fig. 3(b)], a typical Mn^{2+} spectrum of cubic symmetry arises [Fig. 3(d)]. In this new spectrum the six-line hyperfine splitting of $81^{*}10^{-4}$ cm^{-1} is the same as that in the paraelectric phase of $BaTiO_3$.[26] It should be noted that the cubic-symmetry Mn^{2+} spectrum is also visible in samples with lower Nb concentration. However, its intensity is smaller than the intensity of Mn^{2+} tetragonal spectrum, when Nb concentration decreases.[27] Allowing for the fact that Nb impurity at concentration larger than 0.2 at. % decreases the grain size, it is natural to assume that the cubic symmetry Mn^{2+} spectra are formed on the grain boundaries which in posistor $BaTiO_3$ ceramics are well formed and have a marked volume. At the grain boundaries, the tetragonal ferroelectric distortion of the lattice must be much smaller than that inside the grains. In this connection the observed change in the local symmetry of Mn^{2+} impurity is extremely important because it indicates that manganese ions are not uniformly distributed between the grain cores and grain boundaries. At Nb concentration larger than 0.3–0.4 at. %, Mn^{2+} ions can be preferentially located at grain boundaries because here the concentration of Nb ions may be much bigger than in the grains[25] and, therefore, grain boundaries need more Mn^{2+} ions to compensate the excess of positive charge in the lattice. From ESR spectra of Fe^{3+} and Mn^{2+}, it is impossible to distinguish between cubic or rhombohedral symmetry of grain boundaries. The spectrum of Mn^{2+} in the rhombohedral phase ($T<190$ K) in contrast to the tetragonal and orthorhombic phases contains only one visible Mn^{2+} sextet originating from $1/2 \leftrightarrow -1/2$ central transition slightly perturbed by small zero-field crystal field interactions, $b_2^0 \approx (25-50)\times 10^{-4}$ cm^{-1}. The same phenomenon has been observed for Fe^{3+} ions: only one intense line from $1/2 \leftrightarrow -1/2$ central transition is visible. Thus, in the rhombohedral phase the spectra of Fe^{3+} and Mn^{2+} are similar to those in the cubic phase.

With lowering temperature ($T<280$ K—orthorhombic phase and $T<190$ K—rhombohedral phase) the ESR line shape changes in accordance with the crystal symmetry lowering from tetragonal to orthorhombic and rhombohedral, respectively (Fig. 6). It should be stressed that essential decrease of the intensity of Fe^{3+} and Mn^{2+} spectra in $BaTiO_3$ ceramics in the tetragonal and orthorhombic phases in comparison to the intensities in other phases is not related to possible valency charge of these ions due to the trapping of an electron from the conduction band, as was claimed in Refs. 21 and 24. All the intensity changes in the field region of the $1/2 \leftrightarrow -1/2$ transition can simply reflect a redistribution of the spectral intensity from broad magnetic field interval (tetragonal and orthorhombic phases, b_2^0 is large) to narrow magnetic field interval (cubic and rhombohedral phases, b_2^0 is zero or small). This is well seen from Fig. 7, where simulated powder spectra of Fe^{3+} in both the cubic (a) and tetragonal (b) phases are presented. We can also notice that in single crystals there was no evidence that Fe^{3+} and Mn^{2+} spectra change their intensity when the crystal undergoes the phase transitions. However, we cannot exclude that such valency change, at least of Mn ions, occurs at grain boundaries at the tetragonal to cubic transition because even the cubic-symmetry Mn^{2+} spectrum increases in intensity by a factor of 5–6.

From ESR studies of $BaTiO_3$ single crystals it is known that namely the polaronic mechanism is responsible for the capture of the conduction electrons at low temperatures.[9] In Nb-doped $BaTiO_3$ single crystal both polaronic and fluctuonic-type of conduction electron localization were supposed (see sec. III A). In Nb-doped $BaTiO_3$ ceramic samples we also observed ESR spectra of such electrons trapped on host lattice Ti ions. As can be seen from Fig. 6, the Ti^{3+} line with g-factor 1.906 first appears and perfectly coincides with $g_{\perp}$ for Ti^{3+} small polaron center. When the temperature is decreased to 5–4 K, as in the case of single crystals, the spectrum of small polarons decreases in intensity and another Ti^{3+} spectrum appears in the g-factor region 1.89–1.90

(inset to Fig. 6). This g factor approximately coincides with the $g_\perp = 1.890$ of the $Ti^{3+}-Nb^{5+}$ and Ti^{3+} intermediate polarons.[10] Keeping in mind the discussion about the origin of the Ti^{3+} spectra in single crystals in the previous section, one can suppose that Ti^{3+} spectrum in ceramics at $T < 7$ K is related to fluctuon-type of carrier localization. The intensity of these resonances enhances with temperature lowering indicating an increase of the number of localized electrons.

IV. CONCLUSIONS

Our ESR investigations have shown that, in Nb-doped $BaTiO_3$ ceramics and single crystals, electrical conductivity at $T < 300$ K is controlled by electron localization on Ti^{4+} ions—this localization may result in the formation of polarons and/or fluctuons. The latter is related to the observation of a new Ti^{3+} center with $g_x = 1.888$, $g_y = 1.900$, $g_z = 1.928$. This conclusion is valid for single crystals and grain cores in ceramics. In addition, we have shown that the strongly discussed line at $g = 1.971-974$ results from Cr^{3+} centers.

We have also established a segregation of charged centers at grain boundaries in Nb-doped $BaTiO_3$ ceramics. First, for heavy Nb substitutions, the Mn^{2+} and Fe^{3+} spectra were definitely modified. One tetragonal spectrum of Mn^{2+} was ascribed to Mn ions lying in the grain cores because its intensity followed the well-known behavior of bulk materials. On the other hand, a cubic symmetry spectrum appeared in Nb-doped $BaTiO_3$ which we ascribed to grain boundary located centers for the following reasons. In agreement with previous observations, the mean grain size is decreasing on increasing the Nb doping level. At the same time, the cubic Mn^{2+} spectrum intensity continuously increased, thus calling for a link between these centers and the density of grain boundaries. The localization of Mn^{2+} at grain boundaries was further confirmed because of the temperature variation of their ESR spectrum. Indeed, the local environment of Mn^{2+} was found to be nearly cubic without any change between the tetragonal and cubic state of the ceramics. The symmetry at grain boundaries is usually expected to be independent on the tetragonal to cubic phase transition. We thus concluded that Mn^{2+} sites were located at grain boundaries to compensate for the Nb related excess charge. The density of such segregated centers was found to increase at $T > T_c$. Their contribution in the PTCR behavior of $BaTiO_3$:Nb is thus very significant.

ACKNOWLEDGMENTS

This work was financially supported in part by the Project No. 202/02/D078/A GA CR and joint Ukrainian-French project "Dnipro."

[1] W. Heywang, Solid-State Electron. **3**, 51 (1961).
[2] G. H. Jonker, Solid-State Electron. **7**, 895 (1964).
[3] P. Gerthsen and B. Hoffmann, Solid-State Electron. **16**, 617 (1973).
[4] H. Nemoto and I. Oda, J. Am. Ceram. Soc. **63**, 398 (1980).
[5] I. P. Zvyagin and W. Kinase, J. Phys. Soc. Jpn. **54**, 4776 (1985).
[6] T. Miki and A. Fujimoto, J. Appl. Phys. **83**, 1592 (1998).
[7] H. I. Ihrig, J. Am. Ceram. Soc. **64**, 617 (1981).
[8] S. Kohne, O. F. Schirmer, H. Hesse, T. W. Kool, and V. Vikhnin, J. Supercond. **12**, 193 (1999).
[9] R. Scharfschwerdt, A. Mazur, O. F. Schirmer, and S. Mendricks, Phys. Rev. B **54**, 15284 (1996).
[10] S. Lenjer, O. F. Schirmer, and H. Hesse, Phys. Rev. B **66**, 165106 (2002).
[11] C. Gillot, J. P. Michenand, M. Maglione, and B. Jannot, Solid State Commun. **84**, 1033 (1992).
[12] M. D. Glinchuk, I. P. Bykov, S. M. Kornienko, V. V. Laguta, A. M. Slipenyuk, A. G. Bilous, J. Mater. Chem. **10**, 941 (2000).
[13] A. M. Slipenyuk, M. D. Glinchuk, V. V. Laguta, I. P. Bykov, A. G. Bilous, and O. I. V'yunov, Ferroelectrics **288**, 243 (2003).
[14] K. A. Muller, W. Berlinger, and J. Albers, Phys. Rev. B **32**, 5837 (1985).
[15] B. V. Egorov, I. B. Egorova, M. A. Krivoglaz, Fiz. Tverd. Tela (Leningrad) **26**, 3112 (1984), (in Russian); Sov. Phys. Solid State **26**, 1874 (1984).
[16] S. H. Wemple, M. DrDomenico, Jr., and A. Jayaraman, Phys. Rev. **180**, 547 (1969).
[17] T. Sakudo, J. Phys. Soc. Jpn. **18**, 1626 (1963).
[18] T. Sakudo and H. Unoki, J. Phys. Soc. Jpn. **19**, 2109 (1963).
[19] S. M. Kornienko, I. P. Bykov, M. D. Glinchuk, V. V. Laguta, and A. G. Bilous, Fiz. Tverd. Tela (Leningrad) **41**, 1838 (1999), (in Russian); Phys. Solid State **41**, 1688 (1999).
[20] E. Sigel and K. A. Muller, Phys. Rev. B **19**, 109 (1979).
[21] T. R. N. Kutty, P. Murugaraj, and N. S. Gajbhiye, Mater. Lett. **2**, 396 (1984).
[22] G. Er, S. Ishida, and N. Takenchi, J. Mater. Sci. **34**, 4265 (1999).
[23] T. Kolodiazhnyi and A. Petric, J. Phys. Chem. Solids **64**, 953 (2003).
[24] S. Jida and T. Miki, J. Appl. Phys. **80**, 5234 (1996).
[25] S. B. Desu and D. A. Payne, J. Am. Ceram. Soc. **73**, 3407 (1990).
[26] H. Ikushima, J. Phys. Soc. Jpn. **21**, 1866 (1963).
[27] N. Hari, P. Radmini, and T. Kutty, J. Mater. Sci. **8**, 15 (1997).